ORIGINAL REPORT

MJS PUBLISHING

ActaDV Acta Dermato-Venereologica ActaDV Advances in dermatology and venereology

Inhibitory Effect of 505 nm Green Light Emitting Diode on Melanin Synthesis in Cellular Experiments and a Human Intervention Study

Yoshihito MIMA[1], Takehiro YAMADA[1], Jun OMATSU[1], Takashi YAMASHITA[1], Shota SUZUKI[2], Takayuki TAKECHI[2], Mayumi ICHIKAWA[2], Kentaro YAMAZAKI[2], Shinichi SATO[1] and Ayumi YOSHIZAKI[1]
[1]Department of Dermatology, University of Tokyo Graduate School of Medicine, Tokyo, and [2]HYOJO Science Lab, Research and Development Department, YA-MAN Ltd, Tokyo, Japan

Light-emitting diodes (LEDs) are currently gaining attention in aesthetic medicine for their applications in the treatment of pigmentation and wrinkles. While several wavelengths of LEDs have been reported to inhibit melanin production by targeting melanin synthesis-related enzymes, melanosomes, and paracrine factors stimulating melanogenesis from keratinocytes, the effects of green LED (GLED) remain largely unexplored. This study aimed to investigate the effects of GLED on cell viability, melanin production, and melanin-related gene expression using B16 melanoma cells and 3-dimensional (3D) skin models. Furthermore, its efficacy in improving skin pigmentation was evaluated through a human intervention study with GLED-equipped facial masks. The melanin synthesis inhibitory effects of 505 nm GLED were evaluated using B16 mouse melanoma cells, a 3D skin model containing melanocytes, and a human intervention study with 505 nm GLED-equipped masks. 505 nm GLED irradiation reduced melanin production in melanogenesis-induced B16 mouse melanoma cells by suppressing the gene expression levels of microphthalmia-associated transcription factor and tyrosinase. Furthermore, GLED irradiation also reduced melanin content in 3D skin models without affecting cell viability. Finally, a human intervention study demonstrated that GLED irradiation on human facial skin effectively decrease pigmentation. These findings suggest 505 nm GLED is a potential depigmentation strategy.

Key words: 505 nm green light-emitting diode; melanogenesis; tyrosinase; microphthalmia-associated transcription factor; green light-emitting diode-equipped facial masks.

Submitted Mar 22, 2025, Accepted after revision Apr 15, 2025

Published May 15, 2025. DOI: 10.2340/actadv.v105.43441

Acta Derm Venereol 2025; 105: adv43441.

Corr: Ayumi Yoshizaki, Department of Dermatology, University of Tokyo Graduate School of Medicine, 7-3-1 Hongo, Bunkyo-ku, Tokyo 113-8655, Japan. E-mail: ayuyoshi@me.com

SIGNIFICANCE

Light-emitting diodes are increasingly gaining attention in aesthetic medicine for their potential applications in treating pigmentation. However, the effects of green light-emitting diodes remain unexplored. In this study, we demonstrated that 505 nm green light-emitting diodes significantly suppressed microphthalmia-associated transcription factor and tyrosinase expressions, subsequently reducing melanin production not only in melanogenesis-induced B16 mouse melanoma cells but also in 3-dimensional (3D) skin models. Furthermore, the melanin-inhibitory effects of green light-emitting diodes were confirmed in a human intervention study. To our knowledge, this is the first study to suggest that 505 nm green light-emitting diodes may serve as a promising depigmentation strategy in clinical settings.

A light-emitting diode (LED) is a semiconductor device that emits non-coherent, non-collimated, and narrow-band light. LED devices include blue, yellow, red, and near-infrared LEDs, spanning wavelengths between 255 and 1300 nm (1). LEDs are widely used in various applications such as indicators, signage, illumination, data communication, and machine vision systems (2). The light is absorbed by photoreceptive chromophores, subsequently activating these chromophores and altering skin function (3). Furthermore, the high compatibility, convenience, and non-invasive nature of LED technology has led to its wide commercial use in dermatological applications, especially cosmetic dermatology (1–4). This study focuses on the impact of LED therapy on skin pigmentation.

Melanin, derived from the amino acid l-tyrosine, is synthesized via the Raper–Mason pathway through enzymatic and spontaneous reactions (5, 6). In this process, tyrosine is oxidized by tyrosinase (TYR) to form 3,4-dihydroxyphenylalanine, then converted to dopaquinone (7, 8). Moreover, the pathway branches to produce eumelanin and pheomelanin. In the eumelanin pathway, dopaquinone undergoes non-enzymatic conversion to leucodopachrome, which is further transformed into 5,6-dihydroxyindole (DHI) and its derivatives through the action of dopachrome tautomerase (DCT). These intermediates are oxidized and polymerized by tyrosinase-related proteins 1 and 2 (TRP-1 and TRP-2) to form black-to-brown eumelanin (9). In the pheomelanin pathway, cysteine binds to dopaquinone, forming cysteinyldopa, which is oxidized and polymerized into yellow-to-red pheomelanin (6, 9). These pathways are regulated by the microphthalmia-associated transcription factor (MITF),

2025 ©Author(s). Published by MJS Publishing, on behalf of the Society for Publication of Acta Dermato-Venereologica. This is an Open Access article distributed under the terms of the Creative Commons Attribution-NonCommercial 4.0 International License (https://creativecommons.org/licenses/by-nc/4.0/).

ActaDV Acta Dermato-Venereologica ActaDV Advances in dermatology and venereology

which promotes melanogenesis by inducing the enzyme activations of TYR, TRP-1, and TRP-2 through cyclic adenosine monophosphate (cAMP) signals (10, 11). Additionally, α-melanocyte-stimulating hormone (α-MSH) activates the cAMP pathway, increasing MITF expression and subsequently upregulating these enzymes to enhance melanin synthesis (6, 10, 11). Melanin accumulates in lysosome-related organelles known as melanosomes. Mature melanosomes are transferred from melanocytes to neighbouring keratinocytes, resulting in pigmentation (12–14). Abnormal pigmentation results from increased production or reduced degradation of melanin in melanosomes (12–15). This regulated melanogenesis is influenced by genetic factors and enzymatic activity (9, 16–17). While melanosomes and melanin-related factors play critical roles in melanin synthesis, autophagy has been suggested to associate with melanin degradation.

LEDs influence melanin-related enzymes and melanosomes, inhibiting melanin production. Blue LED (BLED) suppresses melanin synthesis and pigmentation in B16 melanoma cells, while yellow LED (YLED) downregulates melanogenesis-related genes and proteins (18, 19). While the effects of LEDs on melanin production at various wavelengths have been researched (18, 19), the impacts of green LED (GLED) on melanin production remain unknown. In this study, we investigated the effects of GLED on melanin production and melanin-related gene expressions by using B16 melanoma cells and 3D skin models. Furthermore, we conducted a human intervention study using GLED-equipped facial masks to assess their effectiveness in improving skin pigmentation on human skin.

MATERIALS AND METHODS

Light sources and irradiation

LED devices with central wavelengths of 450, 505, or 595 nm and cooling fans to minimize temperature elevation were used for irradiation. The LED output was set to 12 mW/cm² for cells and 10 mW/cm² for reconstructed skin models. During cell irradiation, phenol red-free medium was used to minimize light absorption. No temperature increase was observed in the medium or incubator during irradiation.

Cell culture

B16A4 melanoma cells (RIKEN BRC, Ibaraki, Japan) were cultured with DMEM (Wako, Osaka, Japan) supplemented with 10% (v/v) foetal bovine serum (FBS) (Thermo Fisher, Waltham, MA, USA) at 37°C in a humidified atmosphere of air with 5% CO2.

Cell viability assay in B16 melanoma cells

B16 cells were seeded at 0.73×10^4 cells/cm² in 35 mm dishes and incubated overnight. The medium was replaced with fresh media containing 2% FBS, 100 nM α-MSH, and 100 μM theophylline. LED irradiation was performed daily for 3 days. Cell viability was assessed 24 h after the final irradiation using the Cell Count Kit-8 (Dojin, Kumamoto, Japan). Absorbance at 450 nm was measured with a microplate reader (PerkinElmer, Waltham, MA, USA) following the manufacturer's instructions.

Melanin content assay

B16 cells were seeded, cultured, and irradiated in the same manner as described in section 2.3. After B16 cells were washed with PBS (−), cells were dissolved in 1 mol/L sodium hydroxide solution containing 10% DMSO at 85°C for 10 min and divided into 2 aliquots. One was measured at the absorbance of 405 nm for melanin content and the other was measured at the absorbance of 562 nm for protein content using BCA assay (Thermo Fisher, Waltham, MA, USA). The melanin content per unit of cellular protein was calculated and evaluated as the melanin production rate.

Tyrosinase activity assay

Some 24 h after the final irradiation, B16 cells were washed with PBS and lysed in 50 mM phosphate buffer containing 1% Triton X-100, followed by centrifuging at 20,000×g for 10 min. The supernatant was collected like the crude tyrosinase enzyme solution. The supernatant was transferred to a 96-well plate and 5 nM DOPA was added to each well. After incubation for 40 min at 37°C, the absorbance at 475 nm was measured using a microplate reader.

Quantitative real-time PCR analysis

Total RNAs were extracted using the RNeasy Plus Kit (QIAGEN, Venlo, Netherlands) and converted into cDNA using the SuperScript™ IV VILO™ Master Mix (Thermo Fisher, Waltham, MA, USA). Real-time PCR was performed with specific primers to MITF, TYR, TRP1, and TRP2 using the Thermal Cycler Dice® Real Time System IV (Takara Bio, Shiga, Japan). The relative expression of mRNA was calculated by ΔΔCT method and normalized to the expression of GAPDH.

Reconstructed skin model

The melanocyte-containing 3D skin model MEL-300-B was cultured in EPI-100LLMM medium (Kurabo, Japan) for 11 days. The medium was replaced every other day, and LED exposure was performed continuously for 10 days under various irradiation conditions: no irradiation, 10 min, 6 x 10-min sessions, 1 h, and 3 h.

Cell viability assay in 3D skin models

After the final irradiation, MTT assay was performed; 0.5 mg/ml MTT solution (Dojindo, Kumamoto, Japan)

ActaDV Acta Dermato-Venereologica ActaDV Advances in dermatology and venereology

was added to each well. and incubated at 37°C for 3 h. The samples were washed with PBS, immersed in isopropanol, and left overnight to extract formazan. Cell viability was evaluated by measuring the absorbance of the extract at 570 nm.

Melanin content analysis in 3D skin models

The skin models were washed with PBS, subjected to freeze–thaw cycles, and treated with 1% sodium bicarbonate for 30 min. They were then immersed in Solvable™ (Packard BioScience, Meriden, CT, USA) and incubated at 60°C overnight to solubilize melanin. After centrifugation, absorbance at 405 nm was measured for melanin quantification. After 11 days of culture, the skin models were photographed, and the images were binarized and analysed using ImageJ software (National Institutes of Health, Bethesda, MD, USA) to quantify melanin-positive areas.

Histopathological examination of 3D skin models

Samples were fixed in 4% paraformaldehyde, embedded in paraffin, sectioned into 5 µm slices, and stained with haematoxylin and eosin (HE) and Fontana–Masson staining for melanin detection.

Statistical analysis

All data analysis was performed at least 3 times, and the results are expressed as mean ± standard deviation. Statistical significance was determined using Student's *t*-test with EZR software (EZR software). Values of $p<0.05$ (*), $p<0.01$ (**), and $p<0.001$ (***) were considered significantly different.

Human intervention study of GLED

A human intervention study was conducted over 8 weeks to evaluate the effects of a GLED-equipped mask (23F1XX, YA-MAN Ltd, Tokyo, Japan), with one side equipped with GLED and the other side without GLED, on the melanin index, skin brightness (L* value), skin colour index (individual typology angle (ITA) value), and the number of dark spots. The side of the face to which the GLED was applied was randomly assigned, and evaluators were blinded throughout the study to ensure that assessors remained unaware of the allocation. This study was approved by the Pharmaceutical Affairs Expert Committee Ethics Review Board (approval no. 1900186). The trial was conducted under controlled conditions of 21.0 ± 1.0°C and 50.0 ± 5.0% relative humidity. Fifteen healthy female participants aged 45–57 years (mean age: 51.9 ± 3.1 years) were enrolled in the study. Participants continued using their regular skincare products, cleansers, makeup removers, and makeup products. The mask was applied to cleansed, makeup-free skin and used for 10 min, 6 times weekly. Effects were compared between GLED-irradiated and non-irradiated sides. The melanin index was assessed using a Mexameter MX18 (Courage+Khazaka, Cologne, Germany), and L* and ITA value were measured with a spectrophotometer CM-26d (Konica Minolta, Tokyo, Japan), and the number of dark spots was evaluated using the VISIA Evolution (Canfield Scientific, Parsippany, NJ, USA). L* in the CIE Lab colour space represents skin brightness, with higher values indicating a lighter complexion. The individual typological angle (ITA°), calculated from L* and b* values, classifies skin tone, where a higher ITA° indicates a lighter skin colour (20). An increase in L and ITA° suggests improved skin brightness, making them key parameters in skin tone and colour variation research (21, 22). Mexameter MX18 quantifies skin pigmentation density as a melanin index by analysing light absorbance ratios and is widely used in research (23). The measurements were performed 20 min after washing the face. All 4 parameters were evaluated at baseline, week 4, and week 8.

RESULTS

Effects of GLED, YLED, and BLED on the melanogenesis of B16 cells

First, we evaluated GLED's impacts on cell viability, melanin production, and tyrosinase activity. B16 cells were irradiated once daily for three days. No reduction in cell viability was observed (**Fig. 1**A). Melanin production, defined as the melanin-to-protein ratio, decreased in a time-dependent manner, with significant suppression at 7.5 min ($p<0.05$) and 10 min ($p<0.01$) irradiation per day (Fig. 1B). Furthermore, GLED irradiation for 10 min significantly suppressed tyrosinase activity ($p<0.01$), comparable to arbutin (400 µM) with tyrosinase inhibitory effects (24), as a positive control (Fig. 1C). Next, we compared the effects of different LED wavelengths on protein content and melanin production. B16 cells were irradiated with YLED or BLED for 10 min daily over 3 days. GLED and YLED did not alter protein levels, while BLED significantly reduced them, compared with the non-irradiated ($p<0.001$) (Fig. 1D). Under α-MSH and theophylline stimulation, YLED had no effect on melanin production, while GLED significantly reduced it ($p<0.01$), and BLED showed even stronger suppression ($p<0.001$) (Fig. 1E).

Effects of GLED irradiation on melanogenesis-related gene expressions

GLED did not affect cell viability but significantly inhibited melanin production, suggesting its potential for clinical application. To further explore it, we analysed melanin-related gene expression in B16 cells and 3D skin models after GLED irradiation. First, we examined the

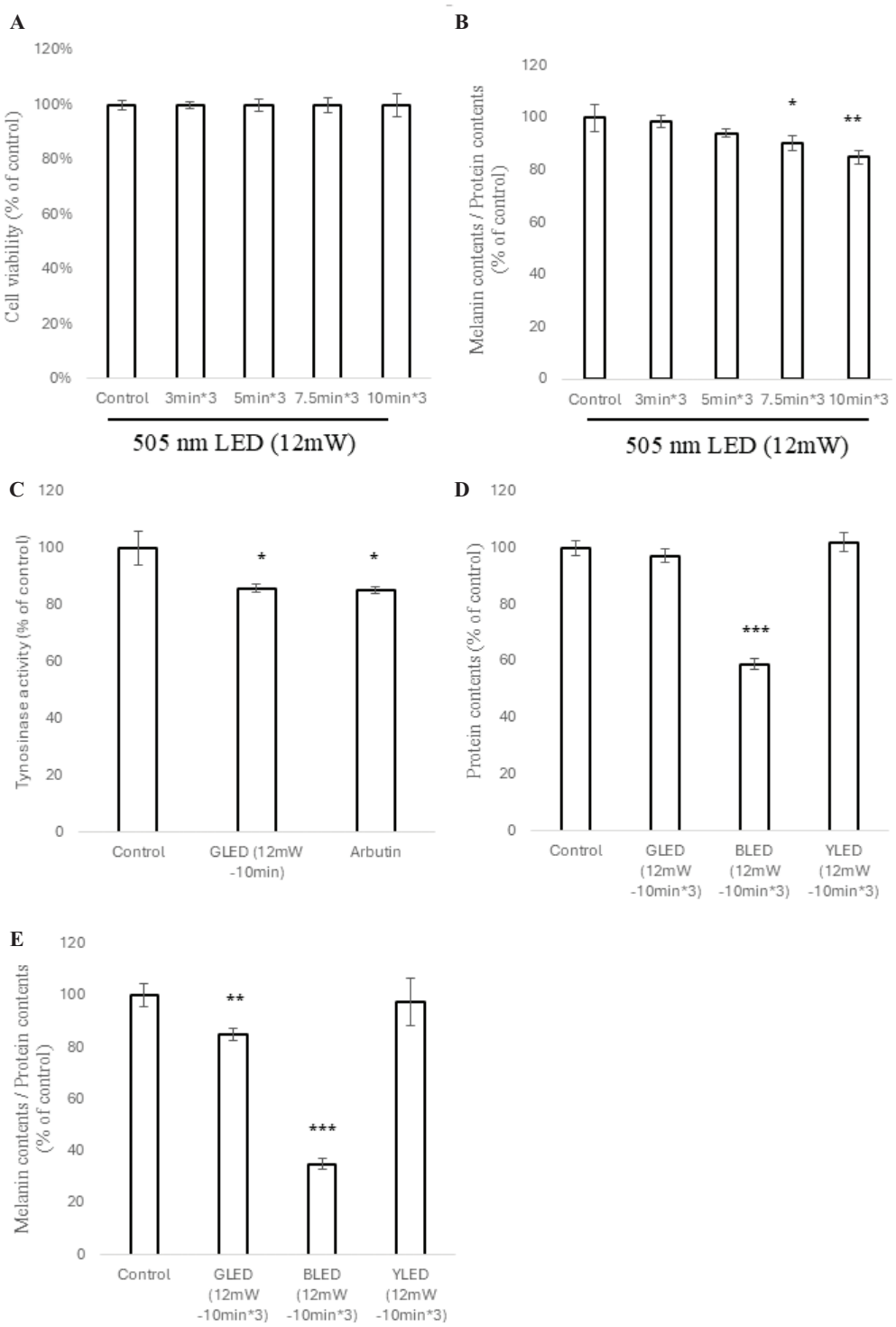

Fig. 1. Effects of GLED, YLED, and BLED on the melanogenesis of B16 cells. (A) Green LED (12 mW/cm²) was applied to B16 mouse melanoma cells once daily for 3 days at durations of 3, 5, 7.5, and 10 min. No reduction in cell viability was observed in any group, as assessed by the WST assay. (B) Green LED (12 mW/cm²) was applied once daily for 3 days to B16 cells stimulated with α-MSH and theophylline to promote melanogenesis, resulting in a time-dependent reduction in melanin production, defined as the ratio of melanin contents to protein contents, with significantly decreased melanin levels observed in the 7.5- ($p < 0.05$) and 10-min ($p < 0.01$) irradiation groups compared with the non-irradiated control. (C) Green LED irradiation (10 min/day for 3 days) on melanogenesis-stimulated B16 mouse melanoma cells significantly suppressed tyrosinase activity ($p < 0.001$) to a level comparable to that achieved with arbutin, a positive control, when compared with the non-irradiated control group. (D) To evaluate the effects of various LED wavelengths on protein contents, B16 cells were exposed to GLED (12 mW/cm²), YLED (12 mW/cm²), and BLED (12 mW/cm²) for 10 min per day over 3 days, and intracellular protein content was measured. YLED, similar to GLED, had no effects on intracellular protein content compared with the non-irradiated control group. In contrast, BLED irradiation led to a significant reduction in intracellular protein contents compared with the non-irradiated control ($p < 0.001$). (E) To evaluate their efficacy, B16 cells were exposed to GLED (12 mW/cm²), YLED (12 mW/cm²), and BLED (12 mW/cm²) for 10 min per day over 3 days, and melanin production was measured. YLED did not exhibit a significant melanin-suppressing effect compared with the non-irradiated control group. In contrast, GLED significantly reduced melanin production ($p < 0.01$), and BLED showed an even greater reduction ($p < 0.001$).

ActaDV Acta Dermato-Venereologica ActaDV Advances in dermatology and venereology

ActaDV Acta Dermato-Venereologica ActaDV Advances in dermatology and venereology

temporal changes of MITF, TYR, TRP-1, and TRP-2 expressions following melanogenesis stimulation without GLED irradiation. MITF peaked 3 h post-stimulation, increasing approximately 2.1-fold, then declined by 6 h and stabilized. In contrast, TYR, TRP-1, and TRP-2 gradually increased over 24 h, with TYR nearly doubling (**Fig. 2**A). Next, B16 cells were irradiated 30 min post-stimulation, and melanin-related gene expression levels were measured at 30 min, 3, 6, and 24 h post-irradiation. The non-irradiated group at each time point was used as the control. As a result, MITF was significantly suppressed as early as 30 min post-irradiation ($p<0.01$), reaching 0.76-fold at 24 h ($p<0.001$). Meanwhile, TYR showed no significant change up to 6 h but decreased to 0.78-fold at 24 h ($p<0.001$), but TRP-1 and TRP-2 remained unchanged (Fig. 2B). Furthermore, to examine the impacts of irradiation timing, GLED was applied 3 h post-stimulation, when MITF peaked. MITF significantly decreased at 3 ($p<0.001$), 6 ($p<0.001$), and 24 hours ($p<0.05$) post-irradiation, reaching 0.91-fold at 24 h. Similarly, TYR significantly decreased at 6 ($p<0.05$) and 24 h ($p<0.01$) post-irradiation, reaching 0.89-fold at 24 h. In contrast, TRP-1 and TRP-2 remained unchanged (Fig. 2C). In both irradiation conditions, MITF and TYR significantly decreased compared with the control, and were significantly higher in the group irradiated 3 h post-stimulation than 30 min post-irradiation ($p<0.01$) (Fig. 2D). Finally, we analysed the time-dependent changes in melanin-related gene expressions following GLED irradiation at 30 min post-stimulation. The control group consisted of non-stimulated B16 cells at each time point. MITF expression peaked at 3 h post-stimulation in both GLED-irradiated and non-irradiated groups, followed by a gradual decline. However, GLED irradiation significantly suppressed MITF at 6 h ($p<0.01$), with even stronger suppression at 24 h ($p<0.001$). TYR increased over 24 h in both groups, but GLED significantly suppressed it at 24 h ($p<0.01$). In contrast, TRP-1 and TRP-2 remained unchanged (Fig. 2E).

Effects of GLED irradiation on the melanogenesis in 3D skin models

To evaluate the effects of GLED on cell viability and melanin contents in 3D skin models, different irradiation conditions were tested: no irradiation, 10 min, 10 min×6, 1 h, and 3 h per day for 10 days. Cell viability remained unaffected across all conditions (**Fig. 3**A), while melanin contents significantly decreased with 10 min×6 ($p<0.01$), 1 h ($p<0.01$), and 3 h ($p<0.001$) per day, showing greater reduction with longer irradiation (Fig. 3B). Additionally, top-down views showed time-dependent decreases in dark areas (Fig. 3C). ImageJ analysis confirmed significant reductions in black pixel counts after 10 min ($p<0.05$), 10 min×6 ($p<0.01$), 1 h ($p<0.001$), and 3 h ($p<0.01$) of daily irradiation (Fig. 3D). Furthermore, HE and Fontana–Masson staining showed reduced pigmentation in the 1-h group compared with controls (**Fig. 3**E).

Human intervention study of GLED mask

A human intervention study using GLED-equipped masks was conducted with randomized, blinded one-sided GLED placement (**Fig. 4**A). After 8 weeks, significant improvements were observed in melanin index ($p<0.001$), skin brightness (L*) ($p<0.001$), skin colour index (ITA°) ($p<0.05$), and the number of spots ($p<0.01$), with all parameters improving over time (Fig. 4B). Clinical photos showed visible enhancements after 8 weeks (Fig. 4C).

DISCUSSION

This study examined melanin-suppressing effects of LEDs. First, BLED, GLED, and YLED were applied to B16 cells to evaluate their effects on intracellular protein contents and melanin production. YLED exhibited no melanin-suppressing effect (Fig. 1E), while BLED significantly inhibited melanin production but reduced intracellular protein levels, potentially impairing cell function (Fig. 1D, E). In contrast, GLED effectively suppressed melanin production without affecting cell viability or protein levels (Figs 1A, D, E). Additionally, GLED irradiation significantly inhibited tyrosinase activity (Fig. 1C), suggesting that its melanin suppression occurs via tyrosinase and related enzymes.

We analysed the effects of GLED irradiation on melanin-related gene expression. First, we examined the temporal changes in MITF, TYR, TRP-1, and TRP-2 following melanogenesis stimulation without GLED irradiation. MITF peaked at 3 h post-stimulation, whereas TYR, TRP-1, and TRP-2 gradually increased up to 24 h (Fig. 2A). These findings align with the theory that α-MSH activates the cAMP pathway, directly inducing MITF activation at 3 h, followed by sequential activation of TYR, TRP-1, and TRP-2 (6, 10, 11). Next, GLED was applied at 30 min and 3 h post-melanogenesis stimulation. In both groups, MITF and TYR significantly decreased 24 h post-irradiation, whereas TRP-1 and TRP-2 remained unchanged (Fig. 2B, C, E). Despite no TRP-1 or TRP-2 suppression, melanin production was markedly reduced in B16 cells. TYR, being upstream in melanin synthesis, may play more crucial roles than TRP-1 and TRP-2 (6–9, 25, 26). In fact, oculocutaneous albinism type 1 (OCA1), caused by TYR mutations, leads to severe skin depigmentation. In contrast, OCA3, resulting from TRP-1 mutations, presents milder hypopigmentation (25, 26). Thus, the significant suppression of MITF and TYR due to GLED irradiation likely accounts for the observed melanin reduction. In both groups of GLED irradiation

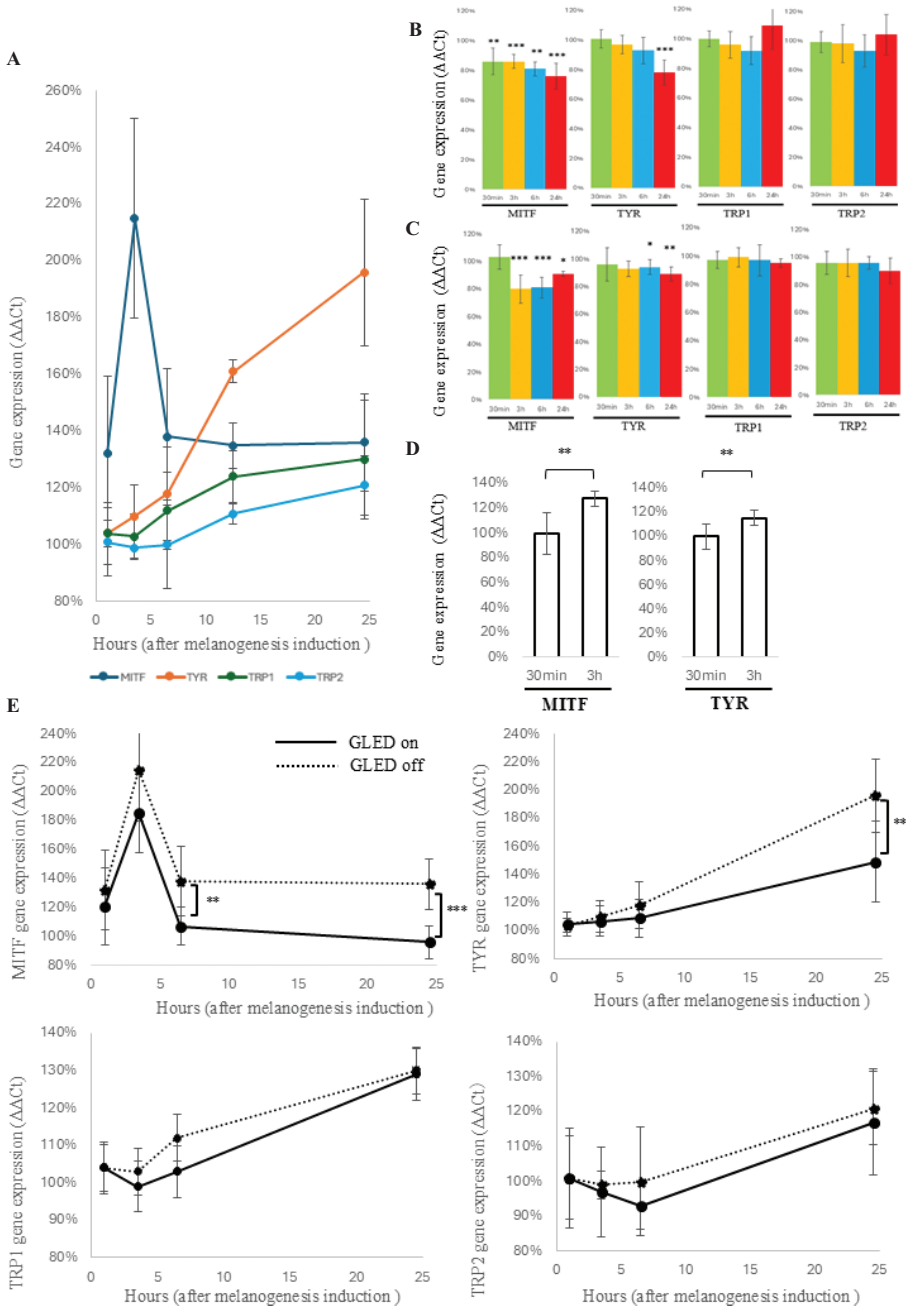

Fig. 2. Effects of GLED irradiation on melanogenesis-related gene expressions. (A) Without green LED (GLED) irradiation, melanogenesis was induced using α-MSH and theophylline, and the time-course changes in MITF, TYR, TRP1, and TRP2 expressions were analysed, using the pre-induction expression levels of each gene as the control. MITF peaked at more than 2.1 times the baseline level at 3 h post-induction, decreased by 6 h, and plateaued up to 24 h. In contrast, TYR, TRP1, and TRP2 increased progressively over 24 h, with TYR showing the most notable rise, reaching nearly twice the baseline at 24 h. (B) GLED irradiation (12 mW/cm²) was applied 30 min after melanogenesis induction, and melanin-related gene expressions were analysed at 30 min, 3 h, 6 h, and 24 h post-irradiation. The control was defined as the expression levels of each gene in the non-irradiated group at the corresponding time points. MITF significantly decreased from 30 min post-irradiation, with the suppressive effect increasing over time. TYR showed no changes at 30 min but exhibited a decreasing trend from 3 h, with significant suppression observed at 24 h. In contrast, TRP-1 and TRP-2 showed no significant changes. (C) GLED (12 mW/cm²) irradiation was applied 3 h after 3 h of melanogenesis induction, and MITF, TYR, TRP-1, and TRP-2 expressions were analysed at 30 min, 3 h, 6 h, and 24 h post-irradiation; MITF showed no change at 30 min due to the strong influence of α-MSH but significantly decreased at 3, 6, and 24 h, TYR significantly decreased after 6 h, while TRP-1 and TRP-2 showed no significant changes. (D) To investigate the difference in the impacts of irradiation timing on melanin-related gene expression, we used the group irradiated with GLED irradiation (12 mW/cm²) 30 min after melanogenesis stimulation as the control and compared gene expression levels at 24 h between this group and the group irradiated 3 h after stimulation. As a result, MITF and TYR were significantly higher in the group irradiated 3 h after stimulation compared with the control (both $p < 0.01$). (E) GLED irradiation (12 mW/cm²) was applied 30 min after melanogenesis induction with α-MSH and theophylline, and the time-course changes in MITF, TYR, TRP1, and TRP2 expression levels were compared with those of the non-irradiated group. The control was defined as the gene expression levels of the non-induced group at each corresponding time point. MITF peaked 3 h after melanogenesis induction and then showed a declining trend, although its effects remained evident at 24 h. However, GLED irradiation significantly reduced MITF expression at 6 and 24 h compared with the non-irradiated group, with expression levels at 24 h decreasing to those of the non-induced group. In contrast, TYR continued to increase up to 24 h after induction. While no significant suppression was observed at 3 and 6 h post-irradiation, a significant reduction was detected at 24 h compared with the non-irradiated group. For TRP-1 and TRP-2, no significant decrease was observed following GLED irradiation.

ActaDV Acta Dermato-Venereologica ActaDV Advances in dermatology and venereology

ActaDV Acta Dermato-Venereologica ActaDV Advances in dermatology and venereology

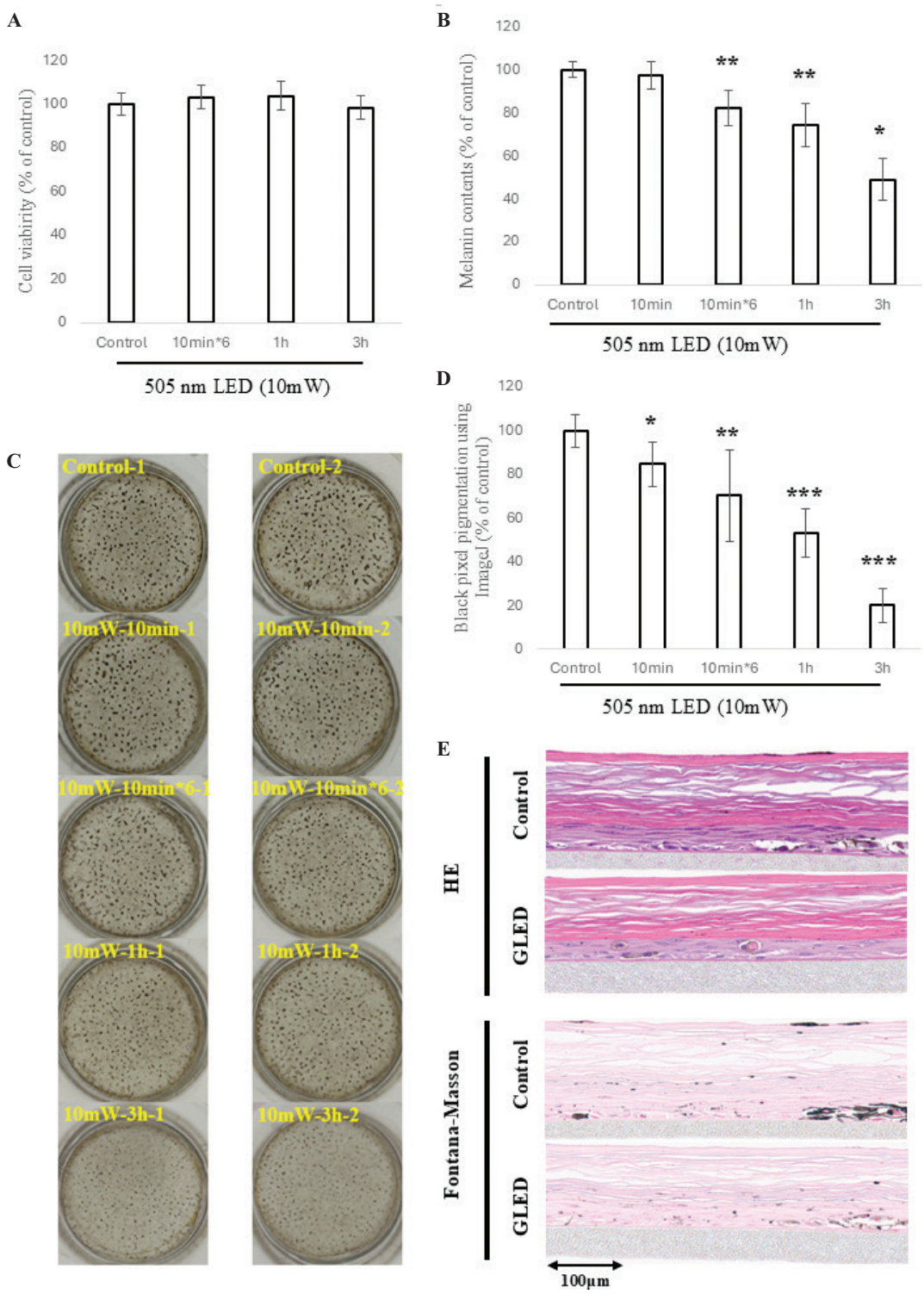

Fig. 3. Effects of GLED Irradiation on the melanogenesis in 3D skin models. (A) Using a 3D skin model, GLED irradiation at 10 mW/cm² was performed under different irradiation conditions, including no irradiation, 10 min, 10 min×6, 1 h, and 3 h per day for 10 consecutive days. Cell viability was evaluated using the MTT assay; no reduction in viability was observed in any group (10 min×6/day, 1 h, or 3 h of irradiation over 10 days) compared with the non-irradiated control. (B) Regarding melanin contents in 3D skin models irradiated with GLED, no significant reduction was observed in the group irradiated for 10 min per day over 10 days. However, significant reductions in melanin content were confirmed in groups irradiated for 10 min×6 ($p<0.01$), 1 h ($p<0.01$), and 3 h ($p<0.001$) per day over 10 days, with longer irradiation durations per session resulting in greater reduction effects. (C) Photographs of the 3D skin model dishes taken from above revealed a visually noticeable reduction in pigmentation in the groups irradiated for 10 min/day, 10 min×6/day, 1 h, and 3 h daily over 10 days, in that order. (D) To assess pigment lightening in 3D skin model dishes, ImageJ was used to evaluate black pixel values. Significant reductions in the proportion of black pixels were observed in all groups irradiated for 10 min, 10 min×6 sessions, 1 h, and 3 h daily for 10 days, with the reduction increasing sequentially in that order. (E) To evaluate the melanin inhibitory effects of GLED, histological observations (HE staining and Fontana–Masson staining) of 3D skin models irradiated with GLED for 60 min per day for 10 days were compared with those of non-irradiated control models. The results showed a visually significant reduction in epidermal melanin pigment in the irradiated group.

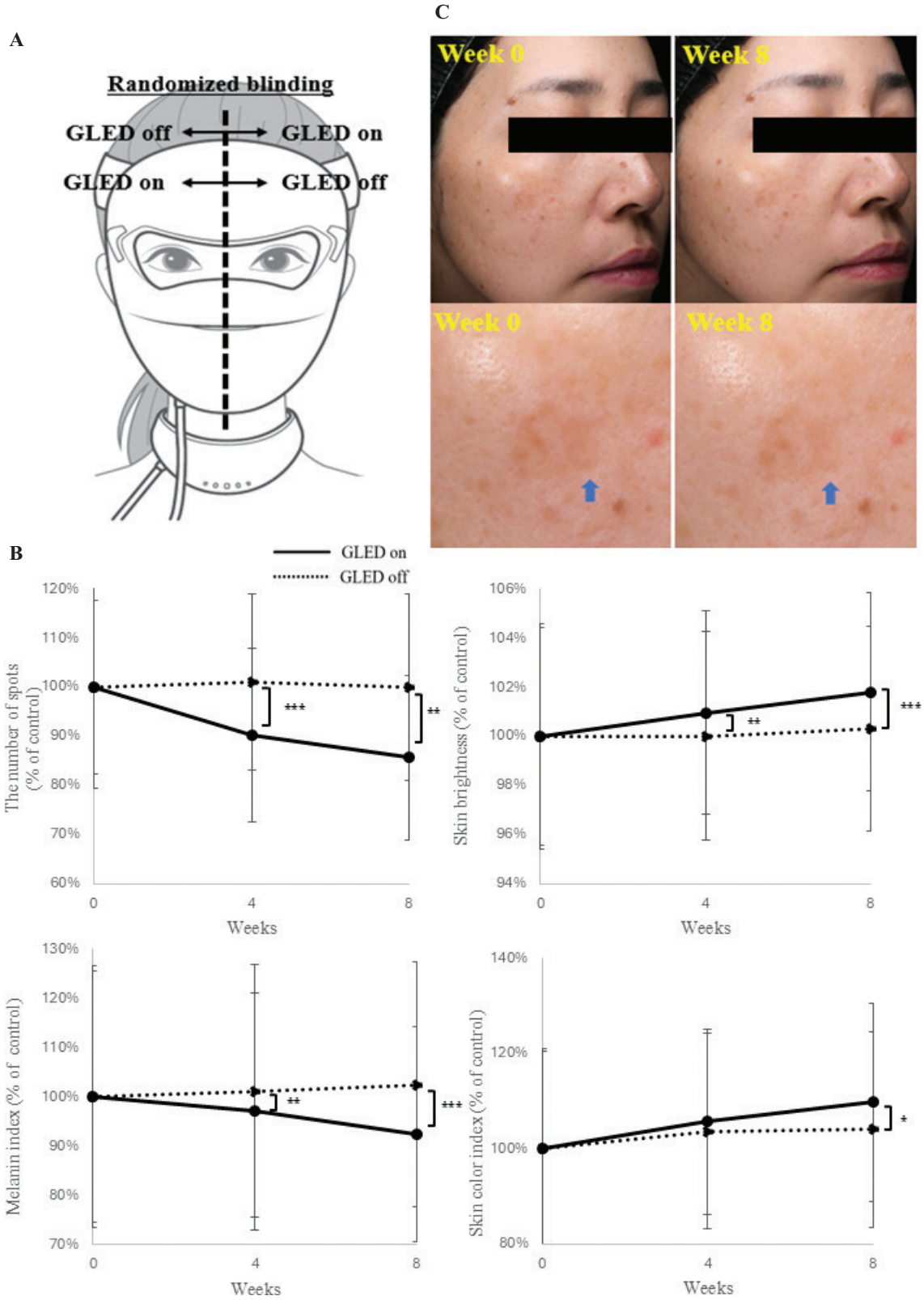

Fig. 4. Human intervention study of GLED mask. (A) We conducted a human intervention study using masks equipped with GLED on 1 side and without GLED on the other, with the placement randomized and blinded to the investigators, to explore its clinical applicability. (B) After 8 weeks of continuous use, the GLED ON side showed significant improvements in all evaluated parameters, including melanin levels ($p < 0.001$), skin brightness ($p < 0.001$), skin colour index ($p < 0.05$), and the number of spots ($p < 0.01$), compared with the LED OFF side. Furthermore, the progression of values at 4 and 8 weeks demonstrated that the longer the irradiation period, the greater the improvement effects observed across all parameters. (C) Clinical photographs, including facial images and magnified views of the cheek area, demonstrated a clear visual improvement in pigmentation and skin transparency after 8 weeks of GLED mask irradiation compared with pre-irradiation (blue arrows).

ActaDV Acta Dermato-Venereologica ActaDV Advances in dermatology and venereology

ActaDV Acta Dermato-Venereologica ActaDV Advances in dermatology and venereology

at 30 min and 3 h post-stimulation, MITF decreased earlier than TYR (Fig. 2B, C), suggesting MITF's role as a master transcription factor. Moreover, when GLED was applied at 3 h post-stimulation, MITF did not significantly decrease at 30 min post-irradiation, unlike in the 30-min irradiation group (Fig. 2B, C), suggesting α-MSH-induced MITF activation outweighed GLED's suppression at that time. To further investigate the impact of irradiation timing, melanin-related gene expressions were compared 24 h after GLED irradiation at 30 min and 3 h post-stimulation. GLED irradiation at 30 min post-stimulation revealed significantly greater suppression of MITF and TYR (Fig. 2D). This suggests that as MITF gradually increases over 3 h following α-MSH stimulation, delayed GLED irradiation may reduce its ability to counteract α-MSH-induced downstream factor activation, thereby weakening MITF and TYR suppression. These findings indicate that early GLED irradiation, such as immediately after sun exposure, may be more effective in clinical applications for suppressing melanin-related gene expression.

Previous studies have utilized 3D skin models to evaluate the efficacy of diode lasers, near-infrared LEDs, and BLED in clinical contents (27–29). This study confirmed that GLED reduces melanin production and related gene expression in B16 cells. Therefore, following previous research (27–29), we further investigated GLED's effects in 3D skin models with melanocytes. GLED irradiation had no impact on cell viability (Fig. 3A) but significantly inhibited melanin production (Fig. 3B). Moreover, its melanin-suppressing effects were validated through ImageJ analysis and histopathological evaluation (Fig. 3D, E).

The efficacy of RLED and near-infrared LEDs on skin wrinkles and elasticity has been reported (30, 31), but GLED has not been studied in humans. Building on GLED's melanin-suppressing effects in the cellular experiments, we conducted a human intervention study using GLED masks (Fig. 4A). Based on GLED's melanin-suppressing effects in B16 cells (Fig. 1B) and reduced pigmentation in 3D skin models via ImageJ analysis (Figs 3C, D), even 10 min of daily irradiation was shown to effectively suppress melanin production. To reflect practical daily use, the human study adopted a 10-min daily irradiation, both achievable and sustainable for regular routines. After 8 weeks, significant improvements were observed in melanin index, skin brightness, skin colour index, and the number of dark spots (Fig. 4B). Although participants used the mask on cleansed and makeup-free skin, GLED may cause hydrogen bonding or hydrogenation reactions (32), and interactions between residual cosmetic ingredients and GLED cannot be fully excluded. This is a limitation of our study.

This study demonstrated that GLED effectively suppressed melanin production by downregulating MITF and TYR in cell experiments and significantly improved facial pigmentation in a human intervention study without adverse events. These findings confirm its potential as a promising treatment for hyperpigmentation. To our knowledge, this is the first human intervention study demonstrating the efficacy of GLED in improving facial pigmentation. Further research and large-scale trials are needed to clarify the melanogenesis mechanisms and therapeutic potential of 505 nm GLED.

ACKNOWLEDGEMENTS

IRB approval status: This study was conducted in accordance with the ethical standards of the institutional and national research committee and with the 1964 Helsinki Declaration and its later amendments or comparable ethical standards. Informed consent was obtained from all individual participants included in the study. All procedures performed in studies involving human participants were in accordance with the ethical standards of HYOJO Science Lab and with the 1964 Helsinki Declaration and its later amendments or comparable ethical standards. This study was approved by the Pharmaceutical Affairs Expert Committee Ethics Review Board (approval 1900186).

The authors have no conflicts of interest to declare.

REFERENCES

1. Barolet D. Light-emitting diodes (LEDs) in dermatology. Semin Cutan Med Surg 2008; 27: 227–238. https://doi.org/10.1016/j.sder.2008.08.003
2. Opel DR, Hagstrom E, Pace AK, Sisto K, Hirano-Ali SA, Desai S, et al. Light-emitting diodes: a brief review and clinical experience. J Clin Aesthet Dermatol 2015; 8: 36–44.
3. Austin E, Geisler AN, Nguyen J, Kohli I, Hamzavi I, Lim HW, et al. Visible light. Part I: Properties and cutaneous effects of visible light. J Am Acad Dermatol 2021; 84: 1219–1231. https://doi.org/10.1016/j.jaad.2021.02.048
4. Wanitphakdeedecha R, Iamphonrat T, Phothong W, Eimpunth S, Manuskiatti W. Local and systemic effects of low-level light therapy with light-emitting diodes to improve erythema after fractional ablative skin resurfacing: a controlled study. Lasers Med Sci 2019; 34: 343–351. https://doi.org/10.1007/s10103-018-2599-1
5. Prota G. The chemistry of melanins and melanogenesis. Fortschr Chem Org Naturst 1995; 64: 93–148. https://doi.org/10.1007/978-3-7091-9337-2_2
6. D'Mello SA, Finlay GJ, Baguley BC, Askarian-Amiri ME. Signaling pathways in melanogenesis. Int J Mol Sci 2016; 17: 1144. https://doi.org/10.3390/ijms17071144
7. Olivares C, Solano F. New insights into the active site structure and catalytic mechanism of tyrosinase and its related proteins. Pigment Cell Melanoma Res 2009; 22: 750–760. https://doi.org/10.1111/j.1755-148X.2009.00636.x
8. Ramsden CA, Riley PA. Tyrosinase: the four oxidation states of the active site and their relevance to enzymatic activation, oxidation and inactivation. Bioorg Med Chem 2014; 22: 2388–2395. https://doi.org/10.1016/j.bmc.2014.02.048
9. Micillo R, Panzella L, Koike K, Monfrecola G, Napolitano A, d'Ischia M. "Fifty Shades" of black and red or how carboxyl groups fine tune eumelanin and pheomelanin properties. Int J Mol Sci 2016; 17: 746. https://doi.org/10.3390/ijms17050746
10. Tachibana M. MITF: a stream flowing for pigment cells. Pigment Cell Res 2000; 13: 230–240. https://doi.org/10.1034/j.1600-0749.2000.130404.x
11. Edelman AM, Blumenthal DK, Krebs EG. Protein serine/threonine kinases. Annu Rev Biochem 1987; 56: 567–613. https://doi.org/10.1146/annurev.bi.56.070187.003031

12. Hearing VJ, Tsukamoto K. Enzymatic control of pigmentation in mammals. FASEB J 1991; 5: 2902–2909. https://doi.org/10.1096/fasebj.5.14.1752358
13. Levy C, Khaled M, Fisher DE. MITF: master regulator of melanocyte development and melanoma oncogene. Trends Mol Med 2006; 12: 406–414. https://doi.org/10.1016/j.molmed.2006.07.008
14. Weiss RA, McDaniel DH, Geronemus RG, Weiss MA. Clinical trial of a novel non-thermal LED array for reversal of photoaging: clinical, histologic, and surface profilometric results. Lasers Surg Med 2005; 36: 85–91. https://doi.org/10.1002/lsm.20107
15. Quevedo WC Jr, Holstein TJ. Molecular genetics and the ontogeny of pigment patterns in mammals. Pigment Cell Res 1992; 5: 328–334. https://doi.org/10.1111/j.1600-0749.1992.tb00557.x
16. Le Pape E, Wakamatsu K, Ito S, Wolber R, Hearing VJ. Regulation of eumelanin/pheomelanin synthesis and visible pigmentation in melanocytes by ligands of the melanocortin 1 receptor. Pigment Cell Melanoma Res 2008; 21: 477–486. https://doi.org/10.1111/j.1755-148X.2008.00479.x
17. Dessinioti C, Antoniou C, Katsambas A, Stratigos AJ. Melanocortin 1 receptor variants: functional role and pigmentary associations. Photochem Photobiol 2011; 87: 978–987. https://doi.org/10.1111/j.1751-1097.2011.00970.x
18. Jin S, Chen L, Xu Z, Xing X, Zhang C, Xiang L. 585 nm light-emitting diodes inhibit melanogenesis through upregulating H19/miR-675 axis in LEDs-irradiated keratinocytes by paracrine effect. J Dermatol Sci 2020; 98: 102–108. https://doi.org/10.1016/j.jdermsci.2020.03.002
19. Ohara M, Kobayashi M, Fujiwara H, Kitajima S, Mitsuoka C, Watanabe H. Blue light inhibits melanin synthesis in B16 melanoma 4A5 cells and skin pigmentation induced by ultraviolet B in guinea-pigs. Photodermatol Photoimmunol Photomed 2004; 20: 86–92. https://doi.org/10.1111/j.1600-0781.2004.00077.x
20. Ly BCK, Dyer EB, Feig JL, Chien AL, Del Bino S. Research techniques made simple: cutaneous colorimetry: a reliable technique for objective skin color measurement. J Invest Dermatol 2020; 140: 3–12. https://doi.org/10.1016/j.jid.2019.11.003
21. Whangsomnuek N, Mungmai L, Mengamphan K, Amornlerdpison D. Efficiency of skin whitening cream containing Etlingera elatior flower and leaf extracts in volunteers. Cosmetics 2019; 6: 39. https://doi.org/10.3390/cosmetics6030039
22. Zamudio Díaz DF, Busch L, Kröger M, Klein AL, Lohan SB, Mewes KR, et al. Significance of melanin distribution in the epidermis for the protective effect against UV light. Sci Rep 2024; 14: 3488. https://doi.org/10.1038/s41598-024-53941-0
23. Watanabe F, Hashizume E, Chan GP, Kamimura A. Skin-whitening and skin-condition-improving effects of topical oxidized glutathione: a double-blind and placebo-controlled clinical trial in healthy women. Clin Cosmet Investig Dermatol 2014; 7: 267–274. https://doi.org/10.2147/CCID.S68424
24. Rudeekulthamrong P, Kaulpiboon J. Optimization of amylomaltase for the synthesis of α-arbutin derivatives as tyrosinase inhibitors. Carbohydr Res 2020; 494: 108078. https://doi.org/10.1016/j.carres.2020.108078
25. King RA, Mentink MM, Oetting WS. Non-random distribution of missense mutations within the human tyrosinase gene in type I (tyrosinase-related) oculocutaneous albinism. Mol Biol Med 1991; 8: 19–29.
26. Manga P, Kromberg JG, Box NF, Sturm RA, Jenkins T, Ramsay M. Rufous oculocutaneous albinism in southern African blacks is caused by mutations in the TYRP1 gene. Am J Hum Genet1997; 61: 1095–1101. https://doi.org/10.1086/301603
27. Riedemann HI, Marquardt Y, Jansen M, Baron JM, Huth S. Biological effect of laser-assisted scar healing (LASH) on standardized human three-dimensional wound healing skin models using fractional non-ablative 1540 nm Er:Glass or 1550 nm diode lasers. Lasers Surg Med 2024; 56: 100–106. https://doi.org/10.1002/lsm.23731
28. Singh S, Escobar A, Wang Z, Zhang Z, Ramful C, Xu CQ. Numerical modeling and simulation of non-invasive acupuncture therapy utilizing near-infrared light-emitting diode. Bioengineering (Basel) 2023; 10: 837. https://doi.org/10.3390/bioengineering10070837
29. Lago JC, Ganzerla MD, Dias ALA, Savietto JP. The influence of blue light exposure on reconstructed 3-dimensional skin model: molecular changes and gene expression profile. JID Innov 2023; 4: 100252. https://doi.org/10.1016/j.xjidi.2023.100252
30. Lee SY, Park KH, Choi JW, Kwon JK, Lee DR, Shin MS, et al. A prospective, randomized, placebo-controlled, double-blinded, and split-face clinical study on LED phototherapy for skin rejuvenation: clinical, profilometric, histologic, ultrastructural, and biochemical evaluations and comparison of three different treatment settings. J Photochem Photobiol B 2007; 88: 51–67. https://doi.org/10.1016/j.jphotobiol.2007.04.008
31. Ng JNC, Wanitphakdeedecha R, Yan C. Efficacy of home-use light-emitting diode device at 637 and 854-nm for facial rejuvenation: a split-face pilot study. J Cosmet Dermatol 2020; 19: 2288–2294. https://doi.org/10.1111/jocd.13613
32. Espinoza JH, Mercado-Uribe H. Visible light neutralizes the effect produced by ultraviolet radiation in proteins. J Photochem Photobiol B 2017; 167: 15–19. https://doi.org/10.1016/j.jphotobiol.2016.11.023

ActaDV Acta Dermato-Venereologica ActaDV Advances in dermatology and venereology